

Hydrologic Response of Grasslands: Effects of Grazing, Interactive Infiltration, and Scale

Fritz R. Fiedler, P.E.¹; Gary W. Frasier²; Jorge A. Ramirez³; and Lajpat R. Ahuja⁴

Abstract: Data collected at two measurement scales from a semiarid grassland are presented and analyzed to explore the hydrologic effects of grazing, interactions between overland flow and infiltration, and scale issues. Rainfall-runoff simulations were used to quantify the areal (3 by 10 m plot scale) response, and small-diameter (9 cm) disk infiltrometers were used to estimate point-scale hydraulic conductivity of bare and vegetated soil. Plot-scale data show that grazing increases runoff overall, a common result, but infiltrometer measurements indicate that only the point-scale hydraulic conductivity of vegetated soil is changed by grazing. In light of this and the well-known relationship between microtopography and vegetation in semiarid grasslands, we hypothesize that small-scale surface interactions (in particular, the so-called run-on phenomenon) are a significant component of the observed effects of grazing, as well as a factor in the hydrologic response of grasslands. Results obtained from high-resolution numerical simulations support this hypothesis. This phenomenon is not captured by classical infiltration theory or by the usual methods of statistical parameterization. In general, interactions are more likely to be important as spatial variability increases, and the relative importance of these interactions will be a function of the spatial structure of the variability and the hydrodynamics of overland flow, as controlled by microtopography.

DOI: 10.1061/(ASCE)1084-0699(2002)7:4(1)

CE Database keywords: Rangeland; Hydrologic aspects; Infiltration.

Introduction

The hydrologic response of watersheds to precipitation is a result of physical processes that occur at many different characteristic scales. Classical point-scale infiltration theory (e.g., the well-known equation of Richards, Green-Ampt, Philip, and Smith-Parlange) is often used in physically based hydrologic models to predict runoff for water use or control engineering, ecological, or pollution control purposes. Researchers have used statistical parameterizations of point-scale model parameters to account for “subgrid” scale spatial variability (Sivapalan and Wood 1986; Blöschl and Sivapalan 1995) based on knowledge of the statistical distribution functions of natural characteristics and assumptions concerning the numerous physical processes controlling the response. Statistical methods are often necessary, due to lack of data and/or computational limitations, and frequently increase our general understanding of the response of complex natural systems.

Existing modeling methodologies have often been used with limited success when applied to natural systems (Michaud and Sorooshian 1994), and poor results can at least in part be attributed to our inability to simply describe, at a large scale, how the many small-scale physical processes interact in the presence of natural spatial variability to produce an integrated response. It is difficult to ascertain the amount of error produced by individual assumptions, and field observations are useful to illustrate the hydrologic process involved. New data, representative of various scales, and analyses thereof can lead to a better understanding of areal hydrologic response. Physically based deterministic models can be used to increase our understanding as well. In this approach, the spatial and temporal scale of discretization must be equivalent to or smaller than the scale of the process to be modeled. While it is not practical at this time to directly simulate small-scale processes in most cases, doing so for research purposes can help ascertain the importance of small-scale interactions to hillslope- and watershed-scale response.

In this paper, we present data collected at two different measurement scales from a semiarid grassland for the purpose of exploring the hydrologic effects of grazing, interactions between overland flow and infiltration, and issues related to scale. These data are used to illustrate the integrated hydrologic response of grasslands at the plot and hillslope scales, and to show how the effects of land-use changes such as grazing might be manifested. We also present results of high-resolution numerical simulations to illustrate the integrated effects of interactions. We conclude that small-scale dynamic interactions between overland flow and infiltration (interactive infiltration) caused by spatially variable soil and ground surface characteristics typical of semiarid grasslands result in an areal hydrologic response not typified by classical point-scale infiltration theory. In interactive infiltration, runoff generated in one area flows to and infiltrates into other areas either during rainfall (run-on) or after rainfall stops, as a result of spatially variable ground surface characteristics or rainfall. It oc-

¹Assistant Professor, Dept. of Civil Engineering, Univ. of Idaho, Moscow, ID 83844-1022.

²Research Hydraulic Engineer, Agricultural Research Service, U.S. Dept. of Agriculture, Crops Research Laboratory, 1701 Center Ave., Fort Collins, CO 80526.

³Associate Professor, Dept. of Civil Engineering, Colorado State Univ., Fort Collins, CO 80523.

⁴Research Leader, Great Plains Systems Research, Agricultural Research Service, U.S. Dept. of Agriculture, Fort Collins, CO 80521.

Note. Discussion open until December 1, 2002. Separate discussions must be submitted for individual papers. To extend the closing date by one month, a written request must be filed with the ASCE Managing Editor. The manuscript for this paper was submitted for review and possible publication on November 6, 2000; approved on December 10, 2001. This paper is part of the *Journal of Hydrologic Engineering*, Vol. 7, No. 4, July 1, 2002. ©ASCE, ISSN 1084-0699/2002/4-1-9/\$8.00+\$0.50 per page.

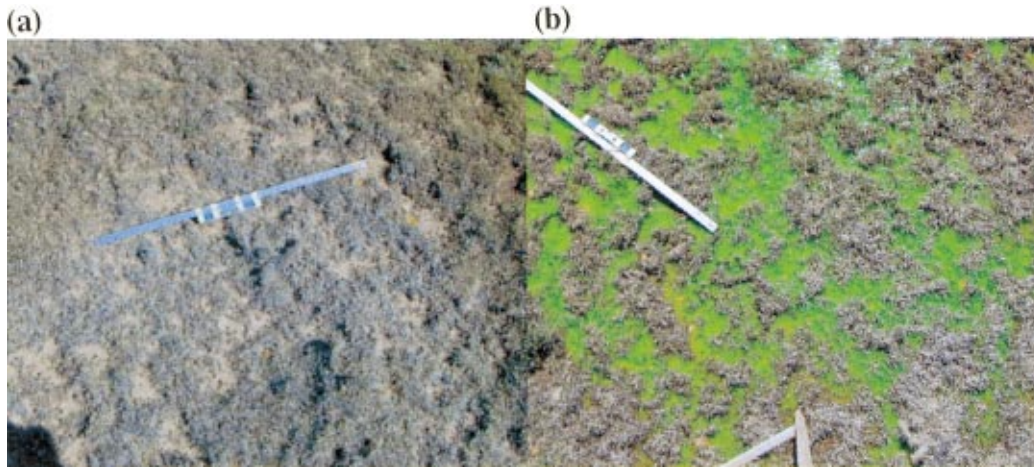


Fig. 1. (Color) Central Plains Experimental Rangeland ground surface: (a) without overland flow; (b) with overland flow (water is dyed bright green and darker vegetation protrudes). A 1-m long ruler is shown for scale.

curs at a variety of scales. Here we only explore how small-scale variability of ground surface characteristics, specifically hydraulic conductivity and microtopography, controls the hydrologic response. These processes are also not accounted for by common statistical treatment of larger-scale model parameters. Additionally, these results suggest that interactive infiltration is at least partially responsible for the observed runoff increases associated with grazing on semiarid grasslands.

Study Area

The study area is located in the Central Plains Experimental Rangeland (CPER), which is approximately 55 km northeast of Fort Collins, Colo. In 1992, a 3 ha enclosure was constructed within each of two neighboring pastures, 23 East and 23 West. These pastures are representative of long-term (approximately 50 years) heavy (LTH) and long-term light (LTL) grazing intensities, respectively. Rainfall-runoff experiments were performed within these enclosures for three years following installation of the enclosures.

The CPER, classified as a short-grass prairie, is in a semiarid region, with an average annual precipitation of 330 mm per year for the last 50 years, and 360 mm per year for the last 10 years, based on unpublished data collected at the site (G. Frasier, personal communication, 1995). This is consistent with the 1961–1990 normal precipitation for the area. Precipitation generally occurs as a result of large convective storms, and as such it is usually localized, and of short duration and high intensity. One-half and 1-h rainfall rates for a 100-year return period are 100 and 75 mm/h, respectively. Median annual maximum rainfall rates for the 1/2- and 1-h durations are 25 and 20 mm/h, respectively (N. Doesken, personal communication, 1995). The hydrologic response of the CPER is characterized by Hortonian runoff generation (infiltration excess), typical of semiarid grasslands. Hillslope gradients are generally small, ranging from 0 to 15%, and the experimental plots have slopes ranging from 2 to 5%, which is typical of much of the short-grass prairie. The soil is an Ascalon sandy loam (Frasier et al. 1995).

The ground surface at the CPER is covered by patchy vegetation, primarily blue grama and buffalo grass. The vegetated-patch size ranges from about 5 up to 50 cm in diameter, with interven-

ing bare patches (interspaces) of similar size; there is often a sharp demarcation between the vegetated and bare patches. Larger (up to several meters) vegetated patches exist, but are laced with smaller bare soil areas. As is commonly observed in semiarid grasslands, vegetated patches strongly correspond to local microtopographic highs, and the bare patches, to lows (Dunne et al. 1991). Fig. 1 shows two pictures of the ground surface at the CPER that exemplify these characteristics. Fig. 1(a) is a picture of the dry ground surface with bare and vegetated patches. Fig. 1(b) is a picture showing overland flow (dyed green for visibility) microchannels.

Small-scale ground surface relief is often referred to as microtopography; however, we have not encountered a working definition of this term as it applies to overland flow. Here, microtopography is defined as *the ground surface topography with approximately the same length scale amplitude and wavelength as the length scale of overland flow depth in a given situation*. This topography causes local flow directions to deviate significantly from the general downslope direction, and the bulk of the flow occurs in small, generally well-defined threads, here termed microchannels. Microrelief amplitude determines the depth of flow that is controlled, and the wavelength affects the size (width) and spacing of the microchannels. The prefix “micro” used in the literature likely evolved from the fact that the topographic relief that affects typical overland flow depths is much smaller in scale (order of centimeters) than the topography associated with commonly available topographical maps (tens of meters). High-resolution microtopographic data were collected from select experimental rainfall-runoff plots with a laser profilometer (Huang and Bradford 1992). At the CPER, the microtopographic amplitude ranges from approximately 2 to 8 cm, and the wavelength is similar to the vegetated-patch size range, i.e., 5–50 cm.

Runoff depth varies greatly in the presence of microtopography, but by definition the microtopographic features are not significantly submerged. Naturally occurring storms in the study area as well as the rainfall rates used in the simulations described subsequently both cause maximum overland flow depths on the order of a few centimeters on short hillslopes. Flow occurs in microchannels ranging in width from 5- to 50-cm wide, which generally weave around microtopographic highs.

Rainfall-Runoff Simulations

Methodology

Areal hydrologic response was quantified by rainfall-runoff simulations performed on 3-m wide by 10-m long rectangular experimental plots during the summers of 1992 through 1995. Four plots in two enclosures (representative of light and heavy grazing treatments) were used each year except in 1995, in which two plots were used in each enclosure. Metal borders installed on three sides served as no-flow boundaries, and outflow was collected and measured at the fourth, the downslope side. A rotating-boom simulator (Swanson 1965) capable of producing two steady rainfall intensities was used to apply water to paired plots; water was sprinkled on two plots at a time, with the simulator located between. Simulations consisted of three phases—low application rate on initially dry soil (DL), low application rate on initially wet soil (WL), and high application rate on initially wet soil (WH). An initial rainfall rate of approximately 60 mm/h (DL) was applied to a relatively dry ground surface for 1 h or until an apparent equilibrium was reached (constant measured outflow). Application was ceased for approximately 1/2 h, then resumed on the wet ground surface (WL) for another 1/2 h or until equilibrium was reached. Finally, the rate was increased to approximately 100 mm/h (WH) for another 1/2 h or until equilibrium was reached. Due to water availability limitations, equilibrium was not always reached at the WL rate before changing to the WH rate, and these runs are not included in the results.

The cumulative depth of the applied water was measured at six locations within each plot during each water application. Artificial rainfall application rates were dividing the average cumulative rainfall amount by the application time over each interval. Outflow hydrographs were measured with calibrated critical depth flumes, and the data were recorded with data loggers at 1 min intervals.

Results

An outflow hydrograph representative of the enclosure in the pasture with historic heavy grazing, along with the corresponding hyetograph, is shown in Fig. 2. This hydrograph, as well as all others, is presented in units of volume rate per unit area. Fig. 3 is representative of the enclosure with historic light grazing condi-

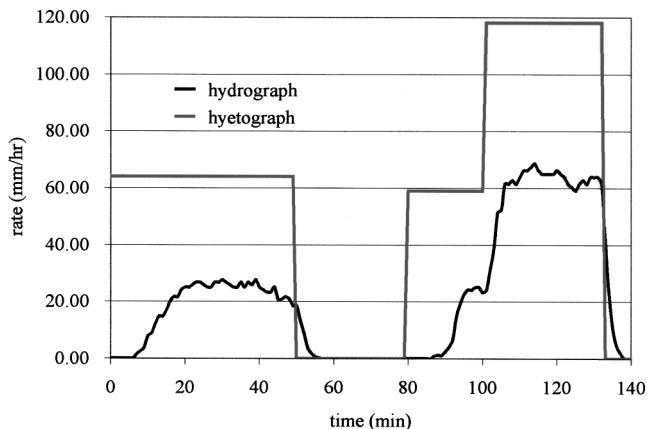


Fig. 2. Representative hyetograph and outflow hydrograph, heavy grazing

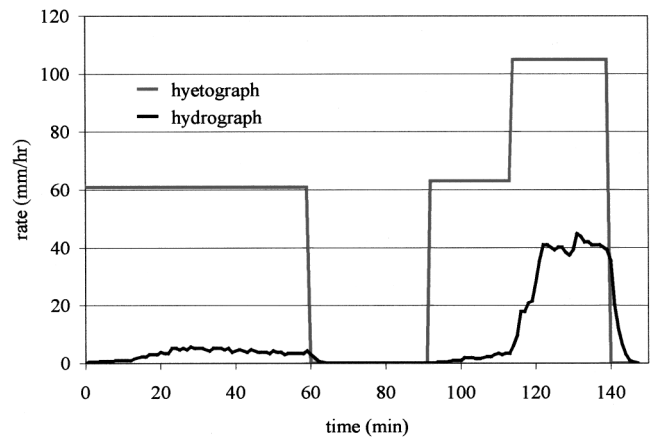


Fig. 3. Representative hyetograph and outflow hydrograph, light grazing

tions. Fig. 4 is a plot of rainfall rate minus outflow rate for the simulation results presented in Fig. 2. At steady state, this graph indicates the plot-averaged, or apparent steady-state infiltration rate. For example, steady state is reached at approximately 20 min for the DL application in Fig. 2. This rate is the integrated response of the plot. The means of the plot-averaged infiltration rates, determined in this manner for each simulation phase and year, are presented in Tables 1 and 2. The results from four plots were used to determine these means, except for 1995, when simulations were only performed on two plots in each treatment. Because the plots are in close proximity to each other, the initial conditions and soil types are very similar (less than 1% difference in gravimetric soil moisture). Also, the results from 23 East in 1994 (items tagged with superscript a in the table) were not used to compute the application phase means because of experimental problems.

Point-Scale Infiltration Measurements

Point-scale generation of excess rainfall occurs when the rainfall rate exceeds the infiltration capacity at a point; this process is also known as Hortonian runoff generation. Therefore, quantification

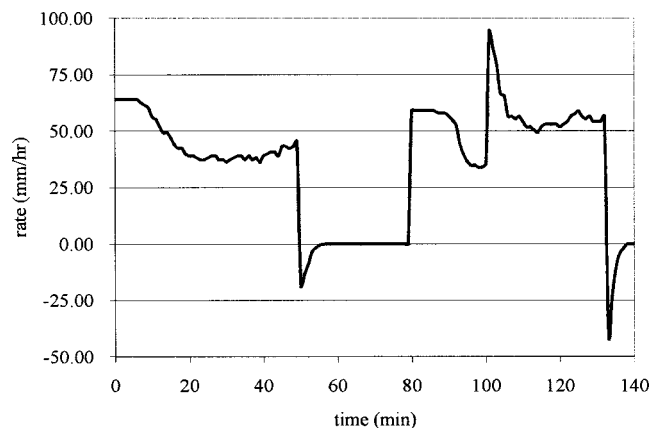


Fig. 4. Rainfall rate minus runoff rate for the data presented in Fig. 2. Note that the negative rate occurs immediately following cessation of rainfall, and continues until surface storage is depleted (runoff stops).

Table 1. 23 West (Long-Term Light Grazing Intensity) Mean Plot-Average Infiltration Rates (mm/h)

Year	DL application phase	WL application phase	WH application phase
1992	54	54	70
1993	54	55	62
1994	57	57	77
1995	52	48	61
[Mean]	54.2	53.5	67.5

Note: The rainfall rates for DL and WL are approximately 60 mm/h; for WH, they were approximately 100 mm/h.

of surface soil infiltration characteristics at some scale is necessary to predict runoff. Quantification of changes in these characteristics is necessary to evaluate the effects of land use changes or land management practices. The word "point" actually refers to a small, elemental volume. When predicting runoff generation with infiltration theory, the smallest elemental volume acceptable depends on the ground surface and soil characteristics, as well as the governing equations. A parameter used in equations to predict infiltration, the hydraulic conductivity, limits the size of the elemental volume to one that contains a sufficient number of pore spaces to make this coefficient valid [the so-called representative elementary volume (REV)]. For example, soils with large pores, such as gravels, require a larger REV than soils with small pores, such as clays. The existence of macropores will affect the smallest admissible REV. In this study, the size of the plots used in the rainfall simulations is much greater than the smallest admissible elemental volume, and the rate of runoff generation varies greatly within the plots. The point-scale infiltration measurement technique used to estimate hydraulic conductivities also encompasses a volume larger than the smallest admissible elemental volume, a necessity for obtaining valid measurements.

Methodology

Steady-state hydraulic conductivities were estimated based on infiltration measurements made with tension infiltrometers (Soil 1992), modified to allow saturated infiltration measurements as well. Briefly, these instruments use a marriot reservoir to control the hydraulic head (tension) at a porous membrane placed at the soil surface, and water flux into the soil at various tensions is measured. To ensure good contact between the porous membrane and the naturally uneven soil surface, a thin layer of contact sand is typically used; this is particularly important on vegetated soil. Good contact is critical for obtaining accurate, reproducible re-

Table 2. 23 East (Long-Term Heavy Grazing Intensity) Mean Plot-Average Infiltration Rates (mm/h)

Year	DL application phase	WL application phase	WH application phase
1992	24	24	35
1993	32	31	40
1994 ^a	34	30	25
1995	42	49	52
[Mean] ^a	32.7	34.7	42.3

Note: The rainfall rates for DL and WL are approximately 60 mm/h; for WH, they were approximately 100 mm/h.

^aThe 1994 results for plots 1 and 2 are not included in the mean.

sults, particularly at higher tensions (Close et al. 1998). Also, the vegetation had to be clipped to allow measurement on vegetated-soil patches. These particular infiltrometers were custom built with small-diameter disks (9 cm) to permit measurement on the small vegetated- and bare-soil patches. Measurements were initially made at 3-, 6-, and 12-cm tensions. The infiltrometers were then modified by the addition of a small ring around the disk which protruded 3 mm into the layer of contact sand, so saturated hydraulic conductivities (using a very slight positive pressure, ~0–1 mm) could be estimated.

Infiltrometer measurements were made at random locations within the rainfall-runoff plots in 1994. In plots located within the heavily grazed enclosure, measurements were made on 14 bare and 17 vegetated patches. In plots located within the lightly grazed enclosure, 10 measurements were made on bare patches, and 10 on vegetated patches.

The analysis technique used in this study is based on a steady-state flux; therefore, data (volume or water infiltrated with time) were collected until an apparent steady state was reached at each tension and location, usually requiring at least 15 min. The final flux rate used to estimate the hydraulic conductivity at each tension and location was determined by a linear regression of the late-time (steady state) data, with time as the independent variable and cumulative infiltrated volume of water as the dependent variable.

Analysis of the disk infiltrometer data relies on the work of Wooding (1968), who assumed an exponential relationship between hydraulic conductivity and matric potential. For a circular surface source of radius

$$Q(\Psi) = \pi r^2 K(\Psi) + 4r\phi(\Psi) \quad (1)$$

where Q , K , and ϕ = flux, hydraulic conductivity, and matric flux potential at the matric potential (tension) Ψ . The matric flux potential is defined as

$$\phi(\Psi) = \int_{\Psi_i}^{\Psi} K(\Psi) d\Psi \quad (2)$$

where Ψ_i = arbitrary (large) tension. The assumed exponential $K(\Psi)$ relationship is

$$K(\Psi) = K_s \exp(\alpha\Psi) \quad (3)$$

where K_s = saturated hydraulic conductivity; and α = a constant dependent on soil type. With these assumptions and definitions, the ratio $K(\Psi)/\phi(\Psi)$ is a constant equal to α . This ratio is substituted into the first equation, leaving Q as a function of K and α .

Linear regression can be used to estimate the parameters of the exponential relationship (K_s and α) if α is assumed to be constant over the range of tensions of interest (i.e., those measured). K values for any tension within the range can then be computed. Eq. (1) and the ratio $K(\Psi)/\phi(\Psi) = \alpha$ are combined to obtain

$$Q(\Psi) = \left[\pi r^2 + \frac{4r}{\alpha} \right] K(\Psi) \quad (4)$$

which is then combined with the logarithmic form of the assumed exponential $K(\Psi)$ relationship

$$\ln[K(\Psi)] = \alpha\Psi + \ln[K_s] \quad (5)$$

to obtain

$$\ln \left[\frac{Q(\Psi)}{\pi r^2 + \frac{4r}{\alpha}} \right] = \alpha\Psi + \ln[K_s] \quad (6)$$

Table 3. 23 East (LTH) Hydraulic Conductivity Data Summary, Lognormal-2 Distribution (mm/h)

Parameter	Scale	Shape	Mean	Median	Mode
$K_B(0)$	-7.4481	0.5634	24.6	21.0	15.3
$K_V(0)$	-5.3589	0.6716	212.4	169.6	108.0
$K_B(3)$	-8.0106	0.4255	13.1	12.0	10.0
$K_V(3)$	-6.8775	0.7085	47.5	37.1	22.5
$K_B(6)$	-8.6420	0.5109	27.2	6.4	4.9
$K_V(6)$	-7.8089	0.6193	17.7	14.6	10.0
$K_B(12)$	-9.1693	0.7367	4.9	3.8	2.2
$K_V(12)$	-8.3391	0.4202	9.4	8.6	7.2

Note: To illustrate the notation, $K_B(0)$ refers to the bare-soil hydraulic conductivity at 0 cm tension. Scale and shape refer to the fitted lognormal distribution parameters.

where α and K_s are unknown. To compute these parameters, the left side of Eq. (6) (for each tension) is estimated using a guess for α , then a regression is performed with these estimated and the known values of Ψ . The computed slope is equal to α , which is then used to recompute the left side, and a second regression is performed with these refined estimates to compute the correct value of the intercept ($\ln[K_s]$). This is the method of Ankeny et al. (1991).

Often, raindrop impact can disrupt the soil surface, thus changing the surface hydraulic conductivity with time during a rainfall event. Clearly, single infiltrometer measurements made at a point cannot be used to quantify this effect. While not presented here because it is beyond the scope of this paper, pairs of infiltration measurements were made at several locations within the plots using the tension infiltrometers before and after removing the top 2–3 mm of soil; no significant difference was found. Observations made during the rainfall simulations showed very little to no sediment movement or change in soil appearance, indicating that rainfall impact was not causing significant soil disruption. If surface sealing did occur, reducing the hydraulic conductivity of the bare soil, the amount of interactive infiltration would increase.

Results

The computed point-scale hydraulic conductivities are separated into four groups—23 East bare soil, 23 East vegetated solid, 23 West bare soil, and 23 West vegetated soil. The spatially variability of the computed point-scale hydraulic conductivity was determined to follow a lognormal probability distribution function, in agreement with previous investigations (Nielsen et al. 1973; Baker and Bouma 1976; Dagen and Bresler 1983). The data are presented in Tables 3 and 4.

Numerical Modeling

Methodology

Distributed, physically based models can, when appropriately discretized, directly simulate the effects of spatial variability and interactions, thus integrating processes across scales. A rainfall-runoff model capable of simulating the complex small-scale flow patterns and interactive infiltration resulting from microtopography and spatially variable infiltration observed at the CPER has been developed (Fiedler 1997). This model is based on the full hydrodynamic overland flow equations, which are necessary for modeling flow over surfaces when the flow depth is of the same

Table 4. 23 West (LTL) Hydraulic Conductivity Data Summary, Lognormal-2 Distribution (mm/h)

Parameter	Scale	Shape	Mean	Median	Mode
$K_B(0)$	-7.2118	0.8315	37.4	26.6	13.3
$K_V(0)$	-5.1289	0.5201	244.1	213.1	162.7
$K_B(3)$	-7.6295	0.5270	20.1	17.5	13.2
$K_V(3)$	-6.0209	0.6175	105.8	87.5	59.8
$K_B(6)$	-8.1950	0.6318	12.1	9.9	6.7
$K_V(6)$	-7.0162	0.4813	36.4	32.2	25.6
$K_B(12)$	-8.8759	0.5988	6.0	5.0	3.5
$K_V(12)$	-7.8865	0.3875	14.6	13.5	11.6

Note: To illustrate the notation, $K_B(0)$ refers to the bare-soil hydraulic conductivity at 0 cm tension. Scale and shape refer to the fitted lognormal distribution parameters.

scale as the small-scale relief, and uses the Green-Ampt infiltration model in a manner that allows fully interactive infiltration. The hydrodynamic equations are solved using a modified MacCormack finite difference scheme, and the Green-Ampt model is solved using Newton-Raphson iterations. Details of the numerical method are published elsewhere (Fiedler and Ramirez 2000). Microtopography is represented within the model by a digital elevation model (DEM) of the plot, obtained using a laser profilometer (Huang and Bradford 1992), at a 2 by 2 cm spatial resolution.

Results

Complete verification of the model used herein is given in Fiedler and Ramirez (2000). Here we show only the results of two rainfall-runoff plot simulations to illustrate that the developed model is capable of reproducing measured data. In the discussion section, additional results are presented to show the importance of interactive infiltration.

The relationship between vegetation and microtopography is represented in the model by a binary distribution of the Green-Ampt infiltration parameters, where parameters representative of vegetated soil are assigned to locally high elevations, and parameters representative of bare soil are assigned to locally low elevations. These parameters, shown in Table 5, were derived from field measurements (K and $\Delta\theta$) and typical values for the CPER soils. The Green-Ampt hydraulic conductivity parameter was taken to be approximately one-half of the measured saturated conductivity. The lognormal distribution mode was used to represent the saturated hydraulic conductivity.

Fig. 5 shows the model results plotted with field experiment measurements obtained in 1993 and 1994 for a representative heavily grazed plot for two different binary distributions of infiltration parameters. Due to potential water repellency of the initially extremely dry soil, which cannot be modeled with the

Table 5. Green-Ampt Infiltration Parameters Used in Numerical Simulations

Parameter	Heavily grazed	Lightly grazed	Heavily grazed	Lightly grazed
	bare soil	bare soil	vegetated soil	vegetated soil
K (mm/h)	7.65	7.65	54.0	82.8
Ψ (mm)	50	50	20	20
$\Delta\theta$	0.04	0.04	0.08	0.08

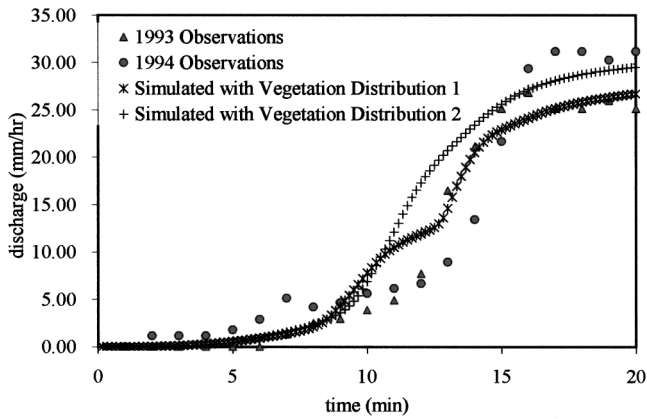


Fig. 5. Simulated and observed plot-scale results for a heavily-grazed plot

Green-Ampt method, the observed data and simulated results are shown for the WL application phase. The distribution of vegetation is the major source of uncertainty in these results, as the actual distribution was not mapped. Both of the simulated distributions were obtained by removing the hillslope trend (macrotopography) from the DEM, and assigning vegetated soil infiltration parameters to elevations above the mean detrended elevation, and bare soil infiltration parameters to elevations below the mean detrended elevation. In this simple but effective manner, the essence of the relationship between microtopography and vegetation is preserved. While both of the simulated distributions visually matched field conditions reasonably well, there are slight differences in the resulting hydrographs.

Discussion

The results of the rainfall-runoff simulations summarized in Tables 1 and 2 show that heavy grazing decreases the apparent steady-state infiltration rates (and thus increases runoff) at both rainfall intensities by over 35%. The physical and hydrological mechanisms giving rise to this observation can be explained, in part, by an analysis of the point-scale data. Model results are also used to support this explanation. It should be noted that these

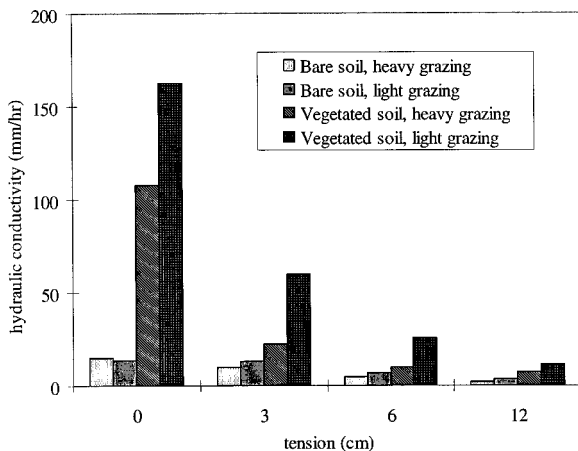


Fig. 6. Lognormal distribution modes of point-scale hydraulic conductivity data

results are interpreted in relation to steady, uniform rainfall and other potential factors such as surface sealing, soil crusting, and water repellency are not considered.

In Fig. 6, the modes of the point-scale hydraulic conductivity data are plotted; in the lognormal distribution, the mode is the measure of central tendency located at the apex of the distribution function. These data illustrate the difference between mean hydraulic conductivities measured at the bare and vegetated patches for both the lightly grazed and the heavily grazed areas near saturation. The differences are smaller for larger tensions, behavior consistent with what is expected due to macropore effects, but clearly bare soil has a lower infiltration capacity. Less obvious are potential differences in point-scale hydraulic conductivities due to the effects of grazing. These differences were statistically evaluated with the Student *t*-test with the log-transformed data. There is no significant difference at the 5% level between bare-soil hydraulic conductivities measured in the lightly grazed and heavily grazed areas at all tensions. However, heavy grazing decreases the hydraulic conductivities of the vegetated soil. There is a significant difference at the 5% level between vegetated hydraulic conductivities at the 12-, 6-, and 3-cm tensions, but not between the saturated (0 cm) values. It should be noted that the high measurement variability at the 0-cm tension likely precluded finding a statistical difference: Fig. 6 illustrates the difference between the modes of the vegetated-soil hydraulic conductivity distributions at 0-cm tension for the different grazing intensities. That grazing primarily impacts vegetated-soil infiltration characteristics, as shown by the point-scale data, is not surprising, since the act of grazing removes vegetation.

Grazing has not occurred in either enclosures since 1992; therefore, the vegetation has had some time to reestablish prior to collection of the point-scale data (collected in 1994). Measurements of the saturated hydraulic conductivity include the effects of macropores, while the measurements made under tension are more representative of the soil matrix. Intuitively, it seems logical that the initial vegetated soil hydraulic conductivity recovery (increase) after the cessation of grazing would be manifested through macropore formation, as plant root systems expand. As time goes on, roots grow and die, decreasing the soil matrix bulk density and increasing porosity, thus increasing the soil matrix conductivity. The results shown here (i.e., no significant difference between the saturated conductivities of vegetated soil) are indicative of a landscape in the process of recovering from the effects of long-term grazing. This is also supported by the rainfall simulation data presented in Table 2, where areal infiltration rates tend to increase with time.

The simulated rainfall rates are significantly greater than the measured bare-soil hydraulic conductivities, and less than or approximately equivalent to the measured vegetated-soil conductivities. During the rainfall-runoff simulations, ponding was visually observed within 3–9 min on bare soil, but the vegetated areas were never completely inundated. Similar bare-soil ponding times were observed on both the lightly grazed and the heavily grazed plots, as expected, given the point-scale hydraulic conductivity measurements. However, as the ponded water encroached upon the vegetation in the lightly grazed plots, the water depth often did not continue to build to the point where significant downslope flow would occur. In all of the plots, vegetation density and therefore hydraulic conductivity vary greatly in space, often with order-of-magnitude differences occurring within distances of less than 10 cm, and are highly correlated with local elevation. Because the bare-soil conductivities are not significantly different between grazing treatments, analysis of the point-scale data indi-

icates that interactive infiltration must be at least partially responsible for how the effects of grazing are manifested.

There is a distinct difference between plot-averaged, steady-state infiltration rates at the low (DL and WL) and high (WH) rainfall intensities. Simulated rainfall rates increased from 70 to 100%, resulting in plot-averaged infiltration rate increases on the order of 25%. At the higher rainfall intensity, the depth of water is greater, thereby inundating more areas of higher hydraulic conductivity (the vegetated areas) and increasing the area over which interactive infiltration can occur. Dunne et al. (1991) modeled this phenomenon in a simplified manner. Thus, the small-scale relationship between microtopography and infiltration characteristics significantly affects the hydrologic response of larger areas, causing areal infiltration rates to be a strong function of rainfall intensity. The exact nature of this relationship for this and other environments has yet to be determined. However, we note that the relationship between infiltration rates and rainfall intensity does not depend on microtopography; it can occur on a plane surface as long as the rainfall intensity is between the minimum and maximum point-scale infiltration capacities.

Using the presented point-scale data to directly predict the areal response is not possible. The point-scale data cannot be simply used (i.e., mean or effective values) to quantify the effects of grazing on the areal hydrologic response, even though there is a measurable difference between vegetated-soil hydraulic conductivities, because of complex interactions resulting from spatially variable ground surface characteristics. It has been shown theoretically that an effective areal hydraulic conductivity can be defined (for simple conceptualization of spatially variable hydraulic conductivity) only after complete ponding of a region (Morel-Seytoux 1986), and nonlinear interactions further obfuscate the concept of an effective conductivity. We expect that the response will be different at larger scales as well, since the greater flow depths associated with longer hillslopes and ephemeral first-order channels will cause greater areal inundation and increase apparent areal infiltration rates. However, this effect may be countered to some degree by increased flow concentrations, which will tend to confine the overland flow to a smaller wetter perimeter.

Traditional methods of statistically parameterizing infiltration models to predict the effects of subgrid variability rely on the assumption that interactions do not occur (Sivapalan and Wood 1986). In general, analysis of this type shows that areal infiltration rates decrease (runoff increases) as the variability of hydraulic conductivity increases; several examples are given in the review by DeCoursey (1996). In our study, we have seen just the opposite; areal infiltration rates were larger in the lightly grazed area, where the difference between bare- and vegetated-soil conductivity is greater (the overall system is more variable). More recently, attempts have been made to account for interactions, albeit in a simple sense where surface flow dynamics are ignored. Nachabe et al. (1997) show that areal infiltration rates are larger when interactions exist, but caution that actual interactions are more complex than the simulated ones. Additionally, Corradini et al. (1998) showed that interactions are important on plane surfaces. Thus, means of incorporating interactions into point-scale hydraulic conductivity upscaling methods need to be developed.

In Fig. 7, four outflow hydrographs are shown. The solid line is the hydrograph produced from a 1 by 1 m surface, with microtopographic relief (measured at the CPER) and hydraulic conductivities spatially distributed in the manner described previously. Saturated hydraulic conductivities of bare and vegetated soil are based on the distribution modes presented in Table 5. The other hydrographs were produced using the same surface, but with uni-

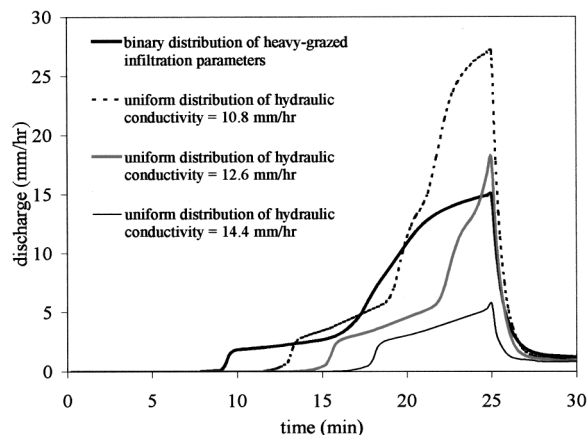


Fig. 7. Discharge hydrographs produced from a surface with microtopographic relief with binary and uniform distributions of hydraulic conductivity

form hydraulic conductivities. The response is such that runoff is produced sooner and the peak is smaller for the distributed case, which is what is expected, given the nature of the distribution and interactive infiltration. Clearly, no single effective conductivity will produce the true response. Physically based distributed hydrologic models typically use point-scale infiltration theory to predict runoff generation using computational grid scales at least as large as the plots used in the rainfall simulations, and should not be expected to produce good results where interactive infiltration is significant. Interactive infiltration can occur whenever Hortonian overland flow occurs. It will become more important as the spatial variability of rainfall, soil moisture, and/or hydraulic conductivity increases. In general, this phenomenon likely plays an underappreciated role in arid and semiarid lands.

Finally, Fig. 8 shows the effects of grazing manifested by interactive infiltration simulated using the model of Fiedler and Ramirez (2000). This simulation utilized the collected microtopographic data. Infiltration model parameters were derived from the point-scale measurements described above and distributed as described previously, and are shown in Table 5. The simulated rainfall rate was 60 mm/h. The *only* difference between the two simulations was that vegetated-soil hydraulic conductivity was

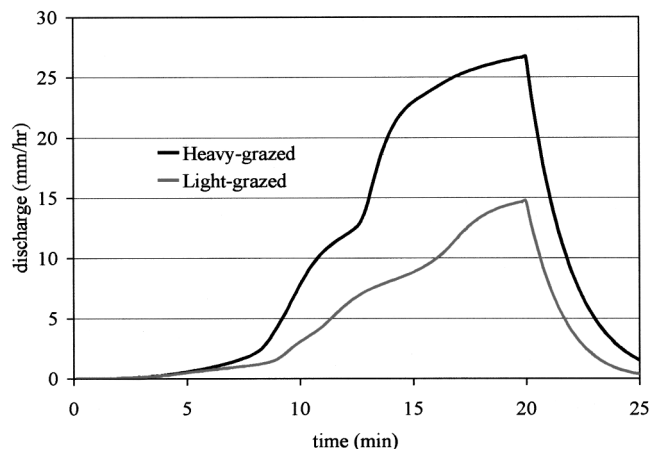


Fig. 8. Simulated effects of grazing. The lightly grazed parameters were based on the values presented in Table 4, and the heavily grazed infiltration parameters were based on the values presented in Table 3.

changed to represent lightly grazed and heavily grazed conditions. In this simulation, differences between the two simulated hydrographs are partially explained by run-on type interactions. Ponding due to rainfall only does not occur given the lightly grazed infiltration parameters, and occurs at approximately 15 min given the heavily grazed infiltration parameters. Therefore, prior to 15 min, the difference is explained completely by surface interactions; after 15 min, the difference is due to interactions as well as rainfall excess generated over the heavily grazed vegetated soil that had not already reached infiltration capacity due to interactions. While there are certainly many other factors that contribute to the hydrologic effects of grazing, we show this result to support the conclusion reached by data analysis, that changes in vegetated-soil hydraulic conductivity caused by grazing can significantly affect the hydraulic response via interactive infiltration.

The presented data show that small-scale dynamic interaction are a significant aspect of the areal hydrologic response at the CPER. It is likely that interactions are important on other grasslands as well, because there is usually a strong relationship between vegetation and microtopography (Dunne et al. 1991). It is yet to be seen whether these interactions are important in other environments. However, we surmise that they are, and that the effects are observed at various scales, which depend on the particular environment.

Conclusions

The foregoing analyses illustrate the importance of surface interactions in areal hydrologic response. Since observations indicate that grazing changes only the vegetated-soil hydraulic conductivity, interactive infiltration is largely responsible for the observed effects of grazing. However, these results do not indicate that interactive infiltration is the only mechanisms through which grazing effects are manifested. Additionally, interactions are almost certainly a major aspect of the hydrologic response of grasslands, and are perhaps more important than indicated by the presented data, due to the effects of bare-soil surface sealing. In fact, grazing may increase surface sealing due to the removal of cover. In the environment described, interactions resulting from the small-scale relationship between microtopography and infiltration characteristics significantly affect the large-scale hydrologic response, causing areal infiltration rates to be a different function of rainfall intensity than would be expected without interactions. In this and other environments, the relative importance of interactions is a function of the spatial structure of the variability and the hydrodynamics of overland flow. Interactions, particularly run-on, are more likely to be important as spatial variability increases. We are not aware of any type of statistical parameterization that could account for the infiltration spatial variability and flow dynamics observed on grasslands, and hope that this work will spur research in this area.

Clearly, more work is needed to identify simple models of Hortonian runoff generation that account for these processes. Statistical parameterizations of point-scale infiltration model parameters, which are sometimes used to model infiltration over large areas, do not account for the spatial structure of variability or the dynamics of overland flow–infiltration interactions. Distributed models can account for spatial variability and integrate processes over scales, but are almost always used with grid cells that are larger than the observed variability, so their usefulness in this regard is not realized. Additionally, it is unlikely that distributed models applied at the watershed scale could directly simulate

small-scale natural variability due to data and computational limitations. We agree with Michaud and Sorooshian (1994), in that parameterization of infiltration processes and identification of dominant processes are research priorities, specifically with respect to the role that surface interactions play in Hortonian runoff generation.

Acknowledgments

The Great Plains Systems Research Unit, Agricultural Research Service, U.S. Department of Agriculture, in cooperation with the Department of Civil Engineering, Colorado State University, supported this work.

References

- Ankeny, M. D., Ahmed, M., Kasper, T. C., and Horton, R. (1991). "Simple field method for determining unsaturated hydraulic conductivity." *Soil Sci. Soc. Am. J.*, 55(2), 467–470.
- Baker, F. G., and Bouma, J. (1976). "Variability of hydraulic conductivity in two subsurface horizons of two silt loam soils." *Proc., Soil Sci. Soc. Am. J.*, Vol. 40, Madison Wis., 219–222.
- Bloschl, G., and Sivapalan, M. (1995). "Scale issues in hydrological modeling: A review." *Scale issues in hydrological modeling*. J. D. Kalma and M. Sivapalan, eds., Wiley, New York, 71–88.
- Close, K. R., Frasier, G., Dunn, G. H., and Loftis, J. C. (1998). "Tension infiltrometer contact interface evaluation by use of a potassium iodide tracer." *Trans. ASAE*, 41(4), St. Joseph, Mich., 995–1004.
- Corradini, C., Morbidelli, R., and Melone, F. (1998). "On the interaction between infiltration and Hortonian runoff." *J. Hydrol.*, 204, 52–67.
- Dagen, G., and Bresler, E. (1983). "Unsaturated flow in spatially variable fields, I. Derivation of models of infiltration and redistribution." *Water Resour. Res.*, 19(2), 413–420.
- DeCoursey, D. G. (1996). "Hydrological, climatological and ecological systems scaling: A review of selected literature and comments." *Interim Progress Rep., USDA-ARS-NPA*, Great Plains Systems Research Unit, Fort Collins, Colo.
- Dunne, T., Zhang, W., and Aubry, B. F. (1991). "Effects of rainfall, vegetation, and microtopography on infiltration and runoff." *Water Resour. Res.*, 27(9), 2271–2285.
- Fiedler, F. R. (1997). "Hydrodynamic simulation of overland flow considering spatially variable infiltration and microtopography." PhD dissertation, Dept. of Civil Engineering, Colorado State Univ., Fort Collins, Colo.
- Fiedler, F. R., and Ramirez, J. A. (2000). "A numerical method for simulation shallow discontinuous flow over an infiltrating surface." *Int. J. Numer. Methods Fluids*, 32, 219–240.
- Frasier, G., Hart, R. H., and Schuman, G. E. (1995). "Rainfall simulation to evaluate infiltration/runoff characteristics of a shortgrass prairie." *J. Soil Water Conservat.*, 50(5), 460–463.
- Huang, C. and Bradford, J. M. (1992). "Applications of a laser scanner to quantify soil microtopography." *Soil Sci. Soc. Am. J.* 56, 14–21.
- Michaud, J., and Sorooshian, S. (1994). "Comparison of simple versus complex distributed runoff models on a midized semiarid watershed." *Water Resour. Res.*, 30(3), 593–606.
- Morel-Seytoux, H. J. (1996). "Influence of variability in hydraulic conductivity on hillslope infiltration." *Proc., 6th Annual AGU Hydrology Days*.
- Nachabe, M. H., Illangasekare, T. H., Morel-Seytoux, H. J., and Ahuja, L. R. (1997). "Infiltration over a heterogeneous watershed: Influence of rain excess." *J. Hydrologic Eng.*, 2(3), 140–143.
- Nielsen, D. R., Biggar, J. W., and Ech, K. T. (1973). "Spatial variability of field-measured soil-water properties." *Hilgardia*, 42(7), 215–259.
- Sivapalan, M., and Wood, E. F. (1986). "Spatial heterogeneity and scale

- in the infiltration response of catchments." *Scale problems in hydrology*, V. K. Gupta, I. Rodriguez-Iturbe, and E. F. Wood, eds., Kluwer Academic, Boston, 81–106.
- Smith, R. E., Goodrich, D. C., Woolhiser, D. A., and Unkrich, C. L. (1995). "KINEROS—A KINematic runoff and EROSION model." *Computer models of watershed hydrology*, V. P. Singh, ed., Water Resources Publications, Littleton, Colo.
- Soil Science Society of America. (1992). "Advances in measurement of soil physical properties: Bringing theory into practice." *Soil Science Society of America Special Publication No. 30*, Madison, Wis.
- Swanson, N. P. (1965). "Rotating-boom rainfall simulator." *Trans. ASAE*, St. Joseph, Mich., 8, 71–72.
- Wooding, R. A. (1968). "Steady infiltration from a shallow circular pond." *Water Resour. Res.*, 4(6), 1259–1273.